Bearing Defect Detection Using Envelope Extraction for Dimension Reduction

Fang Duan, Michael Corsar, Linghao Zhou and David Mba

Abstract Fault detection of the rolling element bearing (REB) has been the subject of extensive research because of its detrimental influence on the reliability of machines. Vibration-based condition monitoring is one of the commonly used methods. In most cases, vibration signals are attenuated and contaminated resulting from background noise and complex structure. Independent component analysis (ICA) has been proved to be an effective method to separate bearing defect related feature from background noise. However, it is a prerequisite that the number of observations has to be larger than that of sources. The requirement cannot be satisfied in helicopter main gearbox (MGB) bearing condition monitoring because it is not possible to install more sensors than vibration sources considering the complexity of the MGB. Hence, this paper investigates the feasibility of using envelope extraction to reduce signal dimension. The experiment was conducted on a MGB operating under different load level and input speed. The results show that bearing defect related feature was observed by combing envelope extraction and the ICA method.

F. Duan (✉) · L. Zhou
School of Engineering, London South Bank University, SE1 0AA London, UK
e-mail: duanf@lsbu.ac.uk

L. Zhou
e-mail: zhoul7@lsbu.ac.uk

M. Corsar
School of Engineering, Cranfield University, MK43 0AL Cranfield, UK
e-mail: m.r.corsar@cranfield.ac.uk

D. Mba
Faculty of Technology, De Montfort University, LE1 9BH Leicester, UK

J. Mathew et al. (eds.), *Asset Intelligence through Integration and Interoperability and Contemporary Vibration Engineering Technologies*, Lecture Notes in Mechanical Engineering, https://doi.org/10.1007/978-3-319-95711-1_14

1 Introduction

Rolling element bearings (REB) are an essential and critical part of rotating machinery. During the service time, faults occurring in bearings may lead to serious damage and fatal breakdown. Hence, REB faults detection and diagnosis in the early stages of damage is necessary to prevent malfunctioning and failure of the whole device. Once bearing defect occurs, a series of impulses are generated every time when a running roller passes over the surface of bearing flaws. As a consequence, the vibration signature of the damaged bearing consists of an exponentially decaying sinusoid having the structure resonance frequency [1]. The amplitude and periodicity of the impulses are related to the structure of bearing, load, flaw location, operating speed and so on. Failures are often preceded by changes in the normal vibration of the system. Therefore, it is feasible to examine the health condition of REBs by monitoring the vibration signals.

Vibration sensors (typically accelerometers) are one of the commonly used sensors in monitoring bearing defects. Since vibrations sensors are normally attached on the case of machine, faults related features are usually immersed in background noise, which makes them difficult to be detected. Over the last few decades, great effects have been made to develop advanced signal processing methods to extract features from signals. Consequently, bearing fault detection methods have been derived from simple calculation of kurtosis and root mean square (RMS) values and Fourier transformation to more sophisticated schemes, such as spectral kurtosis [2], fast kurtogram [3], empirical mode decomposition [4] and independent component analysis (ICA) [5].

Since most gearbox includes multiple vibration sources, the observed vibration signals are the mixtures of different vibration sources. The ICA algorithm has been employed to decompose vibration sources to extract fault related features [5–7]. As one of the general requirements of ICA algorithm, the number of observations should be larger than the number of sources. However, it is not feasible to have more vibration sensors than the vibration sources in the complex MGB scenario. Guo et al. [6] proposed using envelope analysis to reduce dimension prior of using ICA algorithm. The proposed method was validated in a small gearbox with two gears.

So far, most studies were based on simple machinery structures, which have limited number of bearings and gears. In this research, bearing defect detection has been extended from a single bearing to a complex full size helicopter main gearbox (MGB). The MGB consists of several gears and bearings to convert the engine power from high speed and low torque to low speed and high torque to drive the main rotor blades to generate lift. A defect was seeded on one of the planetary gear bearing outer race of the second stage epicyclic reduction gear module. There are multiple vibration sources in the MGB because of the complexity of MGB. Hence, the dimension of recorded vibration signals was firstly reduced by envelope extraction. Then, FastICA algorithm [8] was applied to decompose vibration sources. The experiment was conducted under different rotating speed and load

level. The analysis results proved the efficacy of the combination of the envelope extraction and FastICA in detecting bearing fault in complex environment.

2 FastICA and Envelope Extraction

2.1 FastICA

The FastICA algorithm is a fast and robust fixed-point algorithms for ICA analysis [8]. In our previous study, the FastICA algorithm was employed to separate the multichannel signals into the mutually independent components in the similar scenario [9]. The recorded vibration signals from m accelerometers were regarded as observations $\mathbf{x} = [x_1, \ldots, x_m]$. The FastICA algorithm was utilized to find a mixing matrix A to separate the source signals $\mathbf{s} = [s_1, \ldots, s_i]$. The general ICA model can be expressed as

$$\boldsymbol{x} = A\boldsymbol{s} \tag{1}$$

or equivalent expression of

$$\boldsymbol{s} = A^{-1}\boldsymbol{x} \tag{2}$$

ICA algorithm seeks a matrix W, which has a good approximation of A^{-1}. The FastICA algorithm is based on a fixed-point iteration scheme for finding a maximum of the non-Gaussianity of $\mathbf{w}^T\mathbf{x}$, where $\mathbf{w}$ is the row vector of matrix W. $\mathbf{w}$ can be calculated by using approximate Newton iteration

$$\boldsymbol{w}^+ = \boldsymbol{w} - \mu\left[\mathrm{E}\left\{\mathbf{x}g\left(\boldsymbol{w}^T\mathbf{x}\right)\right\} - \beta\boldsymbol{w}\right] / \left[\mathrm{E}\left\{g'\left(\boldsymbol{w}^T\mathbf{x}\right)\right\} - \beta\right] \tag{3}$$

$$\boldsymbol{w}^* = \boldsymbol{w}^+ / ||\boldsymbol{w}^+|| \tag{4}$$

where $\boldsymbol{w}^*$ and $\boldsymbol{w}^T$ denote the new value and transpose of $\mathbf{w}$, respectively; μ is a step size parameter that may change with the iteration count, $\mathrm{E}\{\cdot\}$ is the mathematical expectation; $g'(\cdot)$ is the derivative of contrast function $G(\cdot)$; $\beta = \mathrm{E}\{\boldsymbol{w}^T\mathbf{x}g(\boldsymbol{w}^T\mathbf{x})\}$. The selection criteria of G and recommended contrast functions can be found in the literature [8]. The algorithm firstly generates $W(0)$ with random elements. Then, the new matrix $W(k)$ is calculated using Eqs. 3 and 4. The algorithm iterates until the value of $I - |W^T(k-1)W(k)|$ is less than a threshold ε or the iteration number k is larger than a given value M.

In that study, the MGB was operated at the high input speed of 16,000 rpm and high loading level of 180 kW. The defect related feature was clearly revealed in one of the independent components spectrum separated by FastICA [9]. However, the FastICA cannot separate the recorded vibration signals when MGB run at low speed and low loading level due to the limited number of vibration sensors. In general, the

number of observations should be larger than the number of sources to have a good separation. However, it is not possible to have more accelerometers than vibration sources in MGB. As an alternative, envelop analysis was employed in this paper to reduce signal dimension to compensate of the limited number of sensors. The envelope analysis method was briefly introduced in the next section.

2.2 Envelope Analysis

Envelope analysis a commonly used method to obtain the bearing defect harmonics from the envelope signal spectrum analysis. The spectral kurtosis (SK) is one of the well-known envelope analysis techniques to detect and characterise transients in a signal. It computes a kurtosis at given frequency resolution in order to discover the presence of hidden non-stationeries and their corresponding frequency bands. The high SK value indicates that the strong impulsive component occurs. The SK can be defined as the fourth-order normalized cumulant

$$k_x(f) = \frac{\left\langle |H(n,f)|^4 \right\rangle}{\left\langle |H(n,f)|^2 \right\rangle^2} - 2, \tag{5}$$

where $H(n, f)$ is the complex envelope of $x(n)$ at frequency f.

Among newly developed envelope extraction methods, the fast kurtogram algorithm, proposed by Antoni [3], is able to compute the kurtogram over finely samples. The high efficiency of the algorithm makes it more suitable for on-line faults diagnosis. In order to increase the calculation efficiency of SK, the fast kurtogram employed binary tree algorithm to split frequency bands. Figure 1 illustrate the kurtogram representation at nodes $\{f_i; \Delta f_k\}$ of the $\{f; \Delta f\}$ plane, which is compounded of $2^K - 1$ kurtosis values.

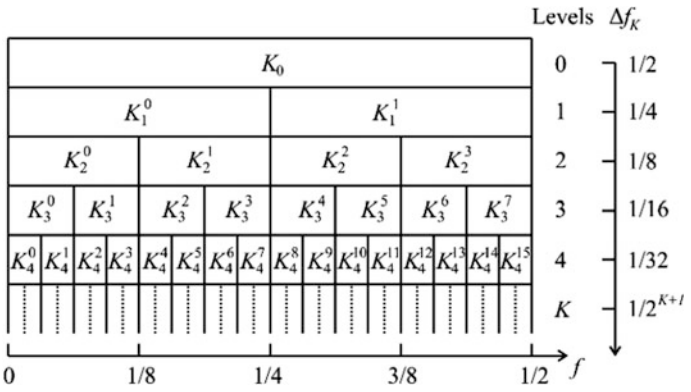

Fig. 1 Sketch of the binary frequency and frequency resolution plane of the fast kurtogram

3 Experiment Rig and Results Analysis

3.1 Experiment Rig

The experiment rig is shown in Fig. 2. The selected CS29 Category "A" SA330 Puma helicopter MGB was mounted on a platform. Flanges at both sides of the platform were designed to support the absorption dynamometer. The absorption dynamometer used air pressure to generate a clamping force between the rotating drive plates driven by the output shaft of the MGB. The level of resistance is proportional to the desired loading on the MGB. Air pressure and flowing water, which was used to remove heat generated by the frictional torque, were delivered to the absorption dynamometer using flexible external tubes.

The MGB consists of five reduction gear modules (RGMs), forward (Fwd) RGMs and after (Aft), left hand (LH) and right hand (RH) RGMs, main RGM and 2-stage epicyclic (Epi) RGM. In the 2-stage Epi RGM, the first and second stage contains 8 and 9 planets gears, respectively. The defect was seeded on one of the planetary gear bearing outer race of the second stage Epi RGM, as shown in Fig. 1b, c. The vibration signals were measured by two PCB triaxial accelerometers (356A32/NC, 100 mV/g). Two accelerometers were located at the case of Epi RGM and Fwd RGM, respectively. The vibration signals were captured by a NI cDAQ-9188XT CompactDAQ data acquisition with sampling frequency of 25.6 kHz.

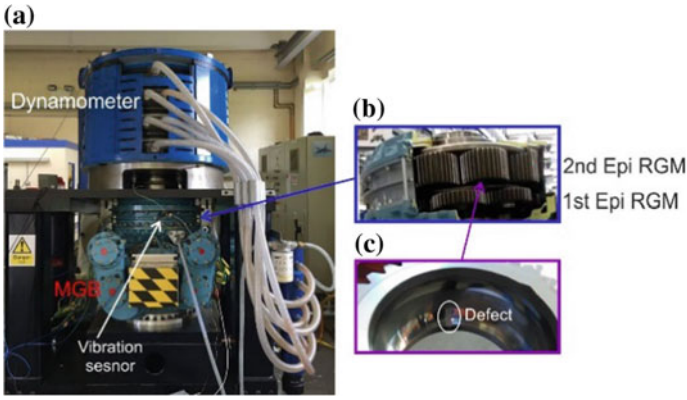

Fig. 2 **a** Experimental rig; **b** 2-stage Epi RGM; **c** Seeded defect at the bearing outer race

3.2 Bearing Defect Detection Methodology

In this study, the experiment was conducted under different loading level and input speed, which were tabulated in Table 1. The seeded bearing defect was simulated by machining a rectangular slot across the bearing outer race with length, width and depth of 10, 4 and 3 mm, respectively. Once bearing outer race defect occurs, the ball impacts on the defect every time when it passes the defect on the outer race. The impact generated vibration can be regarded as a defect signature for fault diagnosis. The defect signature so called bearing outer race defect (ORD) frequency f_{ORD} can be calculated by using

$$f_{ORD} = \frac{N}{2}\frac{S}{60}\left(1 - \frac{d}{D}\cos\alpha\right), \tag{6}$$

where $N = 13$ is the number of rollers; S is planet gear speed of the second stage Epi RGM. $d = 12.5$ mm is the diameter of roller; $D = 63.65$ mm is the pitch diameter and $\alpha = 0$ is the nominal contact angle. The calculated f_{ORD} is equal to 59.88 and 68.55 Hz when the input speed is 14,000 and 16,000 rpm, respectively.

Although the ORD frequency is independent of loading level, the low speed and low loading level made the f_{ORD} difficult to be detected using the FastICA scheme. Therefore, the fast kurtogram algorithm was firstly employed to reduce the dimension of signal.

3.3 Validation and Analysis

Two triaxial accelerometers generate a total six observations. The worst scenario of low input speed of 1400 rpm and low loading level of 100 kW was utilized to illustrate the effectiveness of the combination of two methods. Firstly, the envelopes of seven observations were extracted by the fast kurtogram algorithm. Figure 3a, b show the original vibration signal waveforms of the sensor 1 in tri-axis and their corresponding envelope extracted using the fast kurtogram algorithm. The optimal level and filtering band were set to 7 and 150 Hz, respectively to keep the same length of the envelopes. Although each signal has different optimal level and filtering band, these two values were chosen based on the most common values of

Table 1 Experimental conditions for bearing outer race fault

Input speed (rpm)	Loading level (kW)	BPFO (Hz)
14,000	100	59.88
14,000	180	59.88
16,000	100	68.55
16,000	180	68.55

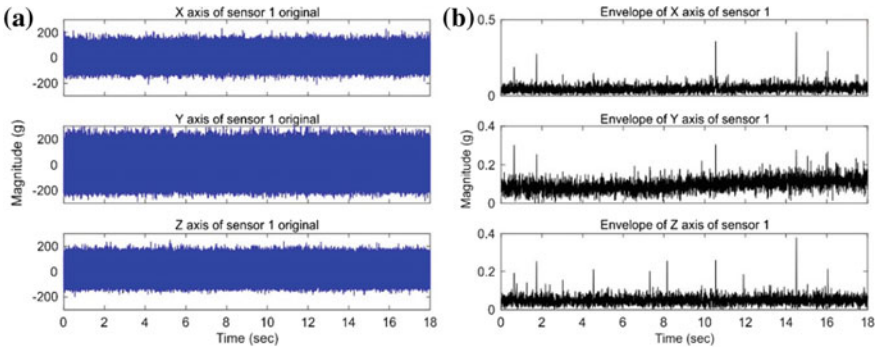

Fig. 3 **a** Original waveforms of sensor 1 in tri-axis; **b** envelope of sensor 1 waveforms in tri-axis

each signal. Similarly, Fig. 4a, b show the original vibration signal waveforms of the sensor 2 in tri-axis and their corresponding envelope.

Finally, the FastICA was utilized to separate vibration sources from 6 mixtures. The separated independent components were transferred from time domain to frequency. The spectrum of these independent components was shown in Fig. 5. Although there was still some mixing frequency components presented in the separation, the defect related feature f_{ORD} of 59.88 Hz was clearly observed in the spectrum of the independent component 4 and 6.

The same procedure was applied to the rest operating condition. The defect related feature f_{ORD} of 59.88 Hz were observed at the spectrum of one of the independent component when the MGB operated at 14,000 rpm input speed, as shown in Fig. 6. Likewise, the defect related feature f_{ORD} of 68.55 Hz were observed at the spectrum of one of the independent component when the MGB operated at 16,000 rpm input speed.

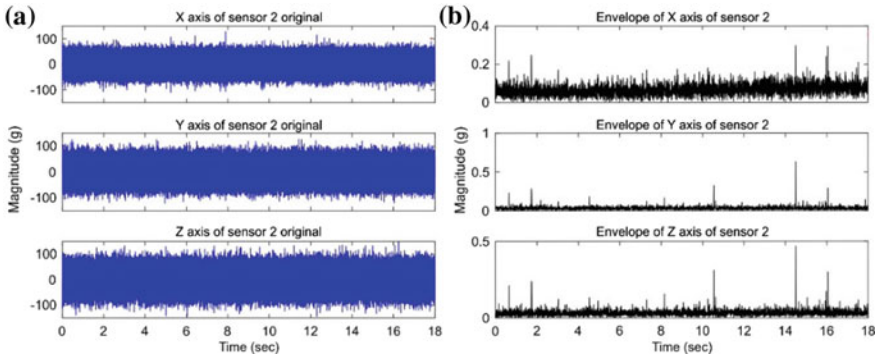

Fig. 4 **a** Original waveforms of sensor 2 in tri-axis; **b** envelope of sensor 2 waveforms in tri-axis

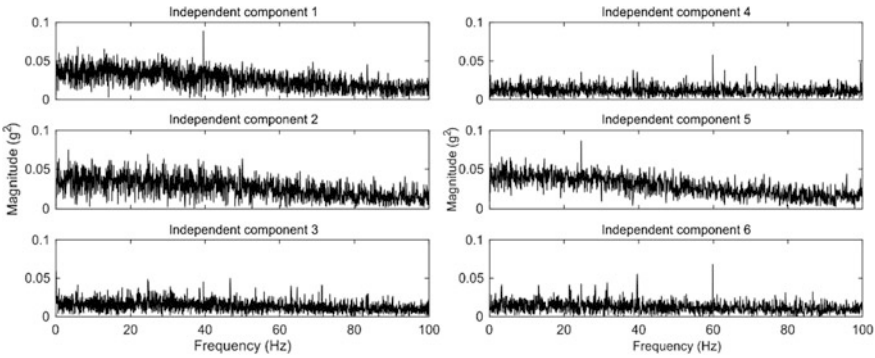

Fig. 5 Spectrum of independent components separated by FastICA

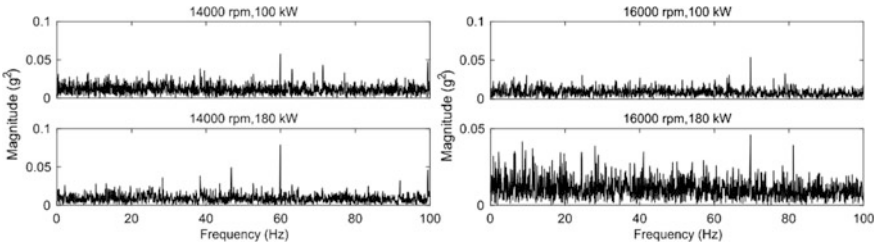

Fig. 6 Independent components including f_{ORD} under different input speed and loading level

4 Conclusion

Since the vibration sensors are usually mounted on the case of helicopter MGB, vibration signal are attenuated and contaminated resulting from strong background noise and multipath transmission. Under these circumstances, it is difficult to extract faults related features from recorded vibration signals. This paper investigates the possibility of combining the fast kurtogram algorithm and the FastICA algorithm to extract faults related features from recorded vibration signals. The fast kurtogram algorithm was firstly utilized to reduced signal dimension to eliminate the constraint of limited number of sensors. Then, the FastICA algorithm was employed to separate vibration sources. The experiment was conducted under different loading level and input speed. In all cases, the defect related feature f_{ORD} was clearly observed at the spectrum of one of the independent component. These results prove the efficacy of the combination of the fast kurtogram algorithm and the FastICA algorithm.

References

1. Stalin S (2014) Fault diagnosis and automatic classification of roller bearings using time-domain features and artificial neural network. Int J Sci Res 3:842–851
2. Wang Y, Liang M (2011) An adaptive SK technique and its application for fault detection of rolling element bearings. Mech Syst Signal Process 25:1750–1764
3. Antoni J (2007) Fast computation of the kurtogram for the detection of transient faults. Mech Syst Signal Process 21:108–124
4. Guo W, Tse PW, Djordjevich A (2012) Faulty bearing signal recovery from large noise using a hybrid method based on spectral kurtosis and ensemble empirical mode decomposition. Measurement 45:1308–1322
5. Ye H, Yang S, Yang J, Ji H (2006) Vibration sources identification with independent component analysis. In 2006 6th World Congress on Intelligent Control and Automation, pp 5814–5818, 0–0 0 2006
6. Guo Y, Na J, Li B, Fung R-F (2014) Envelope extraction based dimension reduction for independent component analysis in fault diagnosis of rolling element bearing. J Sound Vib 333:2983–2994
7. Roan MJ, Erling JG, Sibul LH (2002) A new, non-linear, adaptive, blind source separation approach to gear tooth failure detection and analysis. Mech Syst Signal Process 16:719–740
8. Hyvarinen A (1999) Fast and robust fixed-point algorithms for independent component analysis. IEEE Trans Neural Netw 10:626–634
9. Duan F, Corsar M, Zhou L, Mba D (2017) Using independent component analysis scheme for helicopter main gearbox bearing defect identification. In 2017 Prognostics and System Health Management Conference, Accepted, to be published 2017, pp 1–5